

2D NUMERICAL HEAT INVERSE MODEL FOR DIFFUSIVITY COEFFICIENTS  
IN CARTESIAN COORDINATES

A Thesis

Submitted to School of Graduate Studies and Research

in Partial Fulfillment of the

Requirements for the Degree

Master of Science

Loic Niragire

Indiana University of Pennsylvania

May 2013

Indiana University of Pennsylvania  
School of Graduate Studies and Research  
Department of Mathematics

We hereby approve the thesis of

Loic Niragire

Candidate for the degree of Master of Science

---

Rick Adkins, Ph.D.  
Professor of Mathematics, Advisor

---

Yu-Ju Kuo, Ph.D.  
Associate Professor of Mathematics

---

Majid Karimi, Ph.D.  
Professor of Physics

ACCEPTED

---

Timothy P. Mack, Ph.D.  
Dean  
School of Graduate Studies and Research

Title: 2D Numerical Heat Inverse Model for Diffusivity Coefficients in Cartesian Coordinates

Author: Loic Niragire

Thesis Chair: Dr. Rick Adkins

Thesis Committee Members: Dr. Yu-Ju Kuo  
Dr. Majid Karimi

We investigate the thermal diffusivity property of metal alloys by solving an inverse heat transfer problem using sets of data collected during designed experiments on the heating and cooling of metal alloys. A two-dimensional numerical heat equation is used to model a cross sectional view of the alloys' temperature distribution inside a furnace at any given time. By discretizing the governing equation on a rectangular domain with equal spacing in both x and y directions, diffusivity coefficients are obtained by constructing a series of curves that converges to the actual temperature versus time plot for the alloy in question. A simple explicit scheme is used to advance the solution into the future and boundaries are updated locally while keeping a small time interval between intermediate points.

## ACKNOWLEDGMENTS

I would like to thank all the wonderful teachers and professors who helped me along the way from kindergarten to graduate school.

## TABLE OF CONTENTS

Chapter		Page
1	THE PROBLEM.....	1
	1.1 Background.....	2
	1.2 Solution Overview.....	3
	1.3 Modeling and Significance.....	4
2	REVIEW OF RELATED LITERATURE.....	6
	2.1 The Heat Equation.....	6
	2.2 Harnack Inequality.....	8
	2.3 Finite Difference Discretization .....	9
	2.4 Finite-Element Method.....	13
	2.5 Boundary Element Method.....	14
	2.6 Meshless Methods.....	15
3	METHOD.....	17
	3.1 Results.....	21
	3.2 Conclusion.....	27
	3.3 Endnotes.....	29
REFERENCES	.....	31
APPENDICES	.....	35
	Appendix A – User Interface Notebook.....	35
	Appendix B – Thesis Source Code Notebook.....	40
	Appendix C – Simulation Notebook.....	49
	Appendix D – Navigation Description Notebook.....	53

## LIST OF TABLES

Table		Page
1	Model output for $\alpha = 0.016563$ , $\Delta t = 0.135$ , $dx = 0.1$ for the first point.....	22
2	Model output for $\alpha = 0.016563$ , $\Delta t = 0.135$ , $dx = 0.1$ for the second point .....	23
3	Model output for $\alpha = 0.016563$ , $\Delta t = 0.135$ , $dx = 0.1$ for the third point.....	24
4	Five-Point Scheme with $\Delta t = 0.135$ .....	25
5	Five-Point Scheme with $\Delta t = 0.02$ .....	26

## LIST OF FIGURES

Figure		Page
1	Typical Finite-Difference Grid.....	11
2	Five-point Computational Stencil.....	12
3	Nine-point Computational Stencil.....	12
4	One-Dimensional Finite-Element Mesh.....	13
5	Difference between FEM / FDM Versus Meshless Methods.....	16
6	Specimen Sample.....	17
7	2D Nodal Grid.....	18
8	Initialized 2D Nodal Grid.....	19
9	Temperature vs Time Plot of an Experimental Test.....	21
10	Temperature vs Time Plot for a Five-point Schema with $\Delta t = 0.135$ .....	26
11	Temperature vs Time Plot for a Five-point Schema with $\Delta t = 0.02$ .....	27

## CHAPTER 1

### THE PROBLEM

This thesis is a consequence of a set of curious questions posed by the author while working for a mechanical testing laboratory, Westmoreland Mechanical Testing and Research, in Latrobe Pennsylvania. Question 1: given a particular set-point to for the furnace temperature, how does the accumulated heat at time  $t_i$  affect the overall temperature distribution of the system at time  $t_{i+1}$ ? Question 2: by inserting a metal alloy with unknown thermal properties inside this furnace, does the solution of the first question allow us to learn about the thermal properties of the metal alloy inside the furnace? At first this may seem trivial and that was certainly the case when the author first pondered about these questions. But as it turns out, the implications of these questions have far more reaching applications that go well beyond furnace technology. Some of these applications will be discussed in throughout this thesis. Meanwhile, we explore the above two questions with an emphasis on the second question.

The claim in this thesis is that by understanding temperature propagation inside the furnace and the specimen sample, we can indeed retrieve important materials properties describing its ability to retain heat from its surroundings. One such implication of this is that this knowledge can be used in designing a robust algorithm for temperature ramping. Thus a numerical method for approximating a material's heat diffusivity coefficient at various temperatures is investigated in this thesis. Also, a Mathematica package implementing the suggested method has been developed and is provided in the appendices. We show how, with sufficient

computing resources, material testing laboratories can use existing data to learn about the heat diffusivity of various metal alloys at different temperatures within the tested temperature range. Moreover, the proposed method in this thesis has the ability to run in real time thus providing the ability to reduce energy and time consumption associated with running various material tests at elevated temperature. Although it is worth noting that at the time of writing, the author has made this algorithm run in real time – a topic to be explored further in the future work.

## 1.1

### Background

The topic of heat diffusivity has been studied for a number of years and numerous methods exist for its calculation. Although this thesis does not provide the specifics of material testing procedures for heat diffusivity, the American Society of Testing and Materials provides the most widely used methods. Namely, ASTM E1461-07, "Standard Test Method for Thermal Diffusivity by Flash Method" and ASTM E2585-09, "Standard Practice for Thermal Diffusivity by Flash Method," outline standard specifications used in material testing laboratories and highlight the most commonly used method – Flash Method. One of the known disadvantages of this method is that it is usually expensive and requires special care when it comes to porous and non-homogenous materials. On the other hand, it is very fast and it can be used to measure other thermo-physical properties such as specific heat and thermal conductivity. Note also that the numerical methods in this thesis only address the case of homogeneous materials.

## 1.2

### Solution Overview

The rise of modern computing facilities, from relatively inexpensive terabyte hard drives to high-end processing units and GPU computational capability, made this thesis and its promise possible. Coupled with existing literature on linear partial differential equations of the parabolic type and their numerical treatment, this thesis proposes a method that uses existing temperature distribution data, pertaining to the metal alloy in question, in learning about the heat diffusivity property of the alloy at various temperatures. In the real-time case, collected data up to current time minus  $\psi$  can be used – where  $\psi$  is a specific time determined according to the speed of available computing resources. In other words, with an example set-point of 1200° F, we may collect data to use in our model from the temperature up to 800° F. The assumption here is that enough computing resources will be available to run our model so the results can still be used to control the ramping mechanism for the next short time interval. During this time more data is collected and used to control the next short time interval, and so on. Another critical requirement for the method in this thesis is the ability to sample and record data at a faster rate; the experimental data used in our study were collected at a rate of only two data points per minute – the smaller the time interval the better. As for the computing resources, a high-end processor and large RAM can reduce execution time. This becomes very critical for running the model in real-time. Cloud computing might also be an option. Meanwhile, the provided Mathematica package is very scalable and can be made to run on a set of networked computers. For this thesis, all the work was done on a first

generation i5 Intel processor with 16 GB of RAM and the calculations took a few days depending on the grid size used.

The problem at hand has been approached with a two dimensional model in order to reduce the execution time. The curse of dimensionality can quickly overtake a computers' memory and, if not that, it would take more days to view results. With the promise that we are dealing with homogeneous materials, the three dimensional problem is reduced to two-dimensions by taking a cross-sectional view of the metal alloy in Cartesian coordinates. We propose the five-point finite discrete schema with the heat equation as our governing equation. Note that the five-point finite difference is the recommended method of choice when handling a two-dimensional heat transfer problem under a finite discrete scheme [3].

The goal of this thesis is twofold. First is to provide an analysis tool that scientists and thermal engineers, dealing with material testing and design, can use to learn about heat diffusivity of various metal alloys without a need for extra apparatus or testing routines. The second part is a temperature ramping algorithm than learns in real-time, providing knowledge to control the ramping rate of a furnace.

### 1.3

#### Modeling and Significance

The problem of inferring values of parameters characterizing a system by using data from actual observations is classified as an inverse problem. These problems are among the most challenging in computational science and engineering. In geophysics for instance, one may attempt to determine the distribution of mass inside a planet by measuring its external gravity field. Or in medical imaging, we are

interested in reconstructing an image of something inside the human body from minimally invasive, non-destructive measurements. A German physicist, Viktor Ambartsumian, first studied these problems in 1929. He investigated whether it was possible to find the form of the original equations given a family of eigenvalues.

The non-uniqueness issue associated with the solution of inverse problems is a common factor across disciplines. This has been addressed by the mathematics of ill-posedness and inverse modeling, which formalizes the necessity of bringing additional contextual information to complement a basic theoretical model. This technique is known as regularization, and one of the most widely used regularization techniques is named after a Russian mathematician Andrey Nikolayevich Tikhonov [4]. He is best known in topology where completely regular topological spaces are named Tikhonov spaces.

## CHAPTER 2

### REVIEW OF RELATED LITERATURE

In this chapter we will review some of the most commonly used techniques as they pertain to our problem. An overview of the heat equation is presented and some of the methods used for discretization. A focus is given to the finite-difference, finite-element, boundary element and four of the most used meshless methods. We will also visit the current state of solving  $Ax = b$  in the case where  $A$  is a sparse banded matrix, symmetric also in some cases. Finally, we will wrap up with inverse problems of heat conduction.

#### 2.1

##### The Heat Equation

The heat equation was first proposed by Jean-Baptiste Joseph Fourier (1768-1830) as a mathematical description of the transfer of heat in solid bodies. His motivation was the mathematical study of the diffusion of heat in continuous and solid bodies. His diffusion equation for this purpose was not only novel in itself but also was the first large-scale mathematization of physical phenomena that lay outside mechanics [26]. It provides explanations for such disparate phenomena as the formation of ice, the theory of incompressible viscous fluids, geometric flows, Brownian motion, liquid filtration in porous media, index theorems, the price of stock options and the topology of three-dimensional manifolds.

Propagation of heat is based on a simple continuity principle. The change in the quantity of heat  $u$  in a small volume  $\Delta v$  over a small interval of time  $\Delta t$  is approximately

$$CD \frac{\partial u}{\partial t} \Delta v \Delta t \quad \text{Equation 1}$$

Where  $C$  is the heat capacity of the substance and  $D$  is its density. This change in heat quantity is also given by the amount of heat entering and exiting through  $\Delta v$ , which is approximately

$$K \Delta t \int_{\partial \Delta v} \frac{\partial u}{\partial n} \quad \text{Equation 1}$$

Where  $K$  is the heat conductivity constant and  $n$  is the unit normal to the boundary of  $\Delta v$ . Thus, setting the values of all physical constants to 1, dividing through by  $\Delta t$  and  $\Delta v$ , and letting them tend to zero, we find that the evolution of the amount of heat in a three-dimensional solid  $\Omega$  is governed by the following classical heat equation [26], where  $u(t, X)$  is the temperature at time  $t$  at the point  $X = (x, y, z)$ :

$$\frac{\partial u(t,x)}{\partial t} - \Delta u(t,x) = 0 \quad \text{Equation 2}$$

Where

$$\Delta = \frac{\partial}{\partial x^2} + \frac{\partial}{\partial y^2} + \frac{\partial}{\partial z^2} \quad \text{Equation 3}$$

is the three-dimensional Laplacian. To determine  $u(t, X)$ , the equation (1) needs to be complemented by initial distribution  $u_0(X) = u(0, X)$  and boundary conditions on the solid interface  $\Omega$ . The heat equation has provided numerous explanations to phenomenon across many corners of mathematics.

## 2.2

### Harnack Inequality

The diffusive properties of the heat equation in  $R^2$  are captured by the Harnack inequality for nonnegative solutions  $u$ . This inequality relates the values of a positive harmonic function at two points. In terms of the heat equation, it tells us that

$$\frac{u(t_2, x_2)}{u(t_1, x_1)} \geq \left(\frac{t_1}{t_2}\right)^{\frac{n}{2}} e^{-|x_2 - x_1|^2/(4(t_2 - t_1))} \quad \text{Equation 4}$$

Where  $t_2 > t_1$

This tells us that if the temperature at  $x_1$  at time  $t_1$  takes a certain value, then the temperature at  $x_2$  at time  $t_2$  cannot be too much smaller. This form of Harnack inequality features a very important object in the study of the heat equation, called the heat kernel;

$$p(t, x, y) = \frac{1}{(4\pi t)^{n/2}} e^{-\frac{|x-y|^2}{4t}} \quad \text{Equation 5}$$

It shows that after a time  $t$ , initial point disturbances become distributed in a ball of radius  $\sqrt{t}$  around the point of the original disturbance [26]. This sort of relation between spatial scales and timescales is the characteristic parabolic scaling of the heat equation. Harnack inequality leads to a powerful and simple theorem known as Harnack's principle [29].

This principle applies to a sequence of  $u_n(z)$  functions, each defined and harmonic in a certain region  $\Omega_n$ . It states that if we let  $\Omega$  be a region such that every point in  $\Omega$  has a neighborhood contained in all but finite number of the  $\Omega_n$ , and assume moreover that in this neighborhood  $u_n(z) \leq u_{n+1}(z)$  as soon as  $n$  is sufficiently large. Then there are only two possibilities: either  $u_n(z)$  tends uniformly to  $+\infty$  on every compact subset of  $\Omega$ , or  $u_n(z)$  tends to a harmonic limit function  $u(z)$  in  $\Omega$ , uniformly on compact sets.

## 2.3

### Finite-Difference Discretization

The main idea in the calculus of finite difference is to replace derivatives with

linear combinations of discrete function values. Finite differences have the virtue of simplicity and they account for a large proportion of the numerical methods actually used in applications [28]. The problem domain is first discretized so that the dependent variables are considered to exist at discrete points and then the derivatives are approximated by differences, resulting in an algebraic representation of the underlying partial differential equation. The nature of the resulting equations depends on the character of the problem at hand. To represent a dependent variable  $T$  on a two-dimensional domain spanned by Cartesian coordinates  $(x, y)$ , the continuous function  $T(x, y)$  is replaced by  $T(i \Delta x, j \Delta y)$ . Points can be located according to values of  $i$  and  $j$  so difference equations are written in terms of the general point  $(i, j)$  and its neighbors.

Let us assume the following substitutions:

$$\begin{aligned} T_{i+1,j} &= T(x_0 + \Delta x, y_0) & T_{i-1,j} &= T(x_0 - \Delta x, y_0) & T_{i,j} &= T(x_0, y_0) \\ T_{i,j+1} &= T(x_0, y_0 + \Delta y) & T_{i,j-1} &= T(x_0, y_0 - \Delta y) \end{aligned} \quad \text{Equation 6}$$

By definition of the derivative for the function  $T(x, y)$  at  $x_0, y_0$ :

$$\frac{\partial T}{\partial x} = \lim_{\Delta x \rightarrow 0} \frac{T(x_0 + \Delta x, y_0) - T(x_0, y_0)}{\Delta x} \quad \text{Equation 7}$$

If  $T$  is continuous, it is expected that equation (8) will be a reasonable approximation to  $\frac{\partial T}{\partial x}$  for a sufficiently small but finite  $\Delta x$ . In order to develop the difference approximation, we will use the Taylor series expansion for  $T(x_0 + \Delta x, y_0)$  about  $(x_0, y_0)$ , i.e

$$T(x_0 + \Delta x, y_0) = T(x_0, y_0) + \Delta x \frac{\partial T}{\partial x} + \frac{(\Delta x)^2}{2!} \frac{\partial^2 T}{\partial x^2} + \frac{(\Delta x)^3}{3!} \frac{\partial^3 T}{\partial x^3} + \dots \quad \text{Equation 8}$$

By rearranging equation (9), we can form the forward difference as;

$$\frac{\partial T}{\partial x} = \frac{T(x_0 + \Delta x, y) - T(x_0, y_0)}{\Delta x} - \frac{\Delta x}{2!} \frac{\partial^2 T}{\partial x^2} - \dots \quad \text{Equation 9}$$

Which is equivalent to the following – by applying substitutions found in equation (7)

$$\frac{\partial T}{\partial x} = \frac{T_{i+1,j} - T_{i,j}}{\Delta x} + \mathcal{O}(\Delta x) \quad \text{Equation 10}$$

Backward difference is obtained similarly and is equivalent to:

$$\frac{\partial T}{\partial x} = \frac{T_{i,j} - T_{i-1,j}}{\Delta x} + \mathcal{O}(\Delta x) \quad \text{Equation 11}$$

The second derivative is approximated as:

$$\frac{\partial^2 T}{\partial x^2} = \frac{T_{i+1,j} - 2T_{i,j} + T_{i-1,j}}{\Delta x^2} + \mathcal{O}(\Delta x)^2 \quad \text{Equation 12}$$

Similarly, derivatives are approximated on the y-variable and thus giving a two dimensional representation. Therefore we derive a five-point formula equation representation of Laplaces' equation in two dimensions. This representation is by far the most common difference scheme for the two-dimensional Laplace equation [3];

$$\frac{T_{i,j+1} - 2T_{i,j} + T_{i,j-1}}{\Delta y^2} + \frac{T_{i+1,j} - 2T_{i,j} + T_{i-1,j}}{\Delta x^2} = 0 \quad \text{Equation 13}$$

With a truncation of  $\mathcal{O}(\Delta x)^2 + \mathcal{O}(\Delta y)^2$

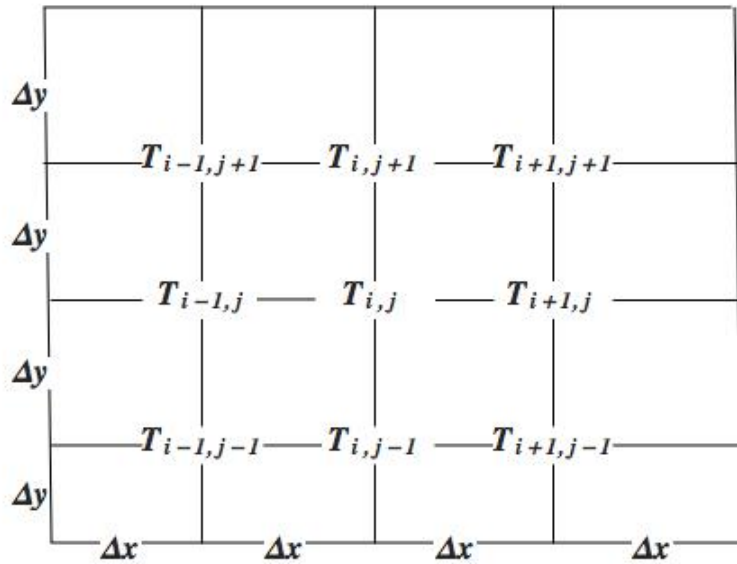


**Figure 1** Typical Finite-Difference Grid [3]

Equation (14) can be rewritten as:

$$T_{i,j+1} + T_{i,j-1} + T_{i+1,j} + T_{i-1,j} - 4T_{i,j} = (\Delta x)^2 f_{i,j} \quad \text{Equation 14}$$

Where  $f_{i,j} = f(x_0 + i \Delta x, y_0 + j \Delta x)$

Another way to depict equation (14) is via a computation stencil as:

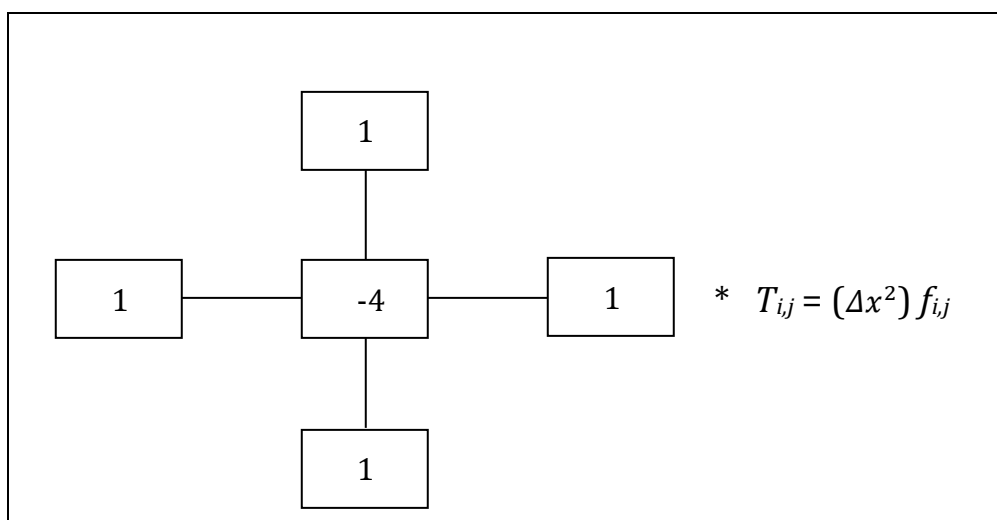


**Figure 2** Five-Point Computational Stencil

One of the alternatives to the five-point formula is to use eight nearest neighbors: horizontal, vertical and diagonal. This results in the nine-point formula depicted as following:

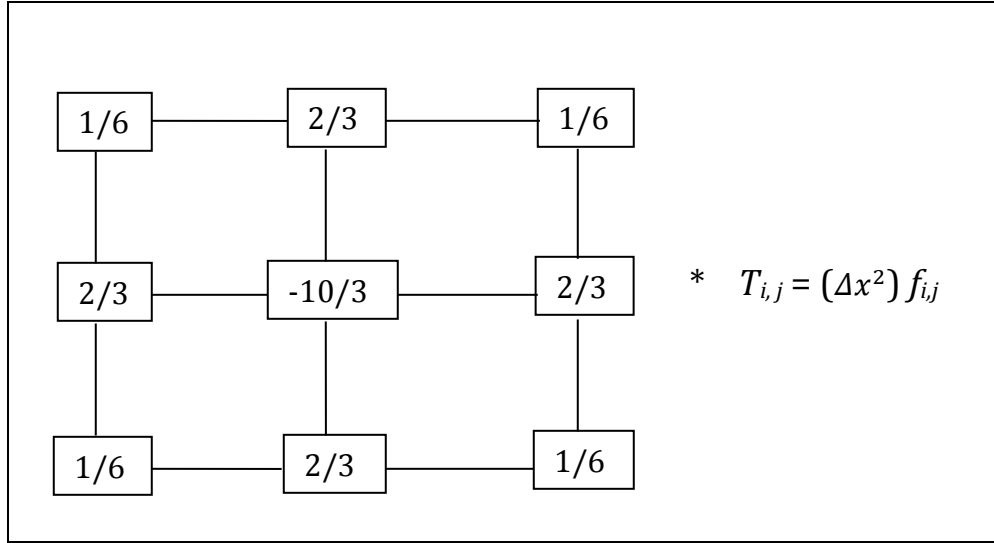


**Figure 3** - Nine-point Computational Stencil

However, nothing is gained by incorporating the diagonal neighbors as we end up with a truncation error of  $\nabla^2 + \frac{1}{12}(\Delta x)^2 \nabla^4 + \mathcal{O}(\Delta x^2)$  which is exactly the same order of magnitude as that of the five-point formula [28].

## 2.4

### Finite-Element Method

The finite element method (FEM) was first developed to analyze aero structures in the late 1950s [13]. Its potential for use in thermal analysis and fluid flow was also quickly recognized, and the first implementations appeared in the mid-1960s [14]. It replaced the original function by a function which has some degree of smoothness over the global domain, but which is piecewise polynomial on simple cells, such as triangles or rectangles. One preferred method of developing the FEM is the use of the

Rayleigh-Ritz variational formulation, which lends itself to the development of a rich mathematical theory but requires the existence of a minimum principle [15]. This presentation is based on the Galerkin-weighted residuals formulation, which allows for the formulation of problems when minimum principles do not exist and therefore can be extended to cover convective heat transfer and fluid flow [16].

The first step in FEM is to subdivide the domain over which the equation is to be solved into a number of subdomains, which are called elements. The end points of the elements are called nodes. In one dimension, the elements are simple subintervals, as shown in Fig. 1 with four elements. The partition of the interval must satisfy two conditions: (1) the union of all elements must be equal to the whole interval, and (2) the elements cannot overlap. The second step in FEM is to represent any function  $f(x)$  defined over  $0 \leq x \leq L$  as a piecewise function that interpolates the original function at the nodes and has a prescribed form in the interior of the elements as shown below

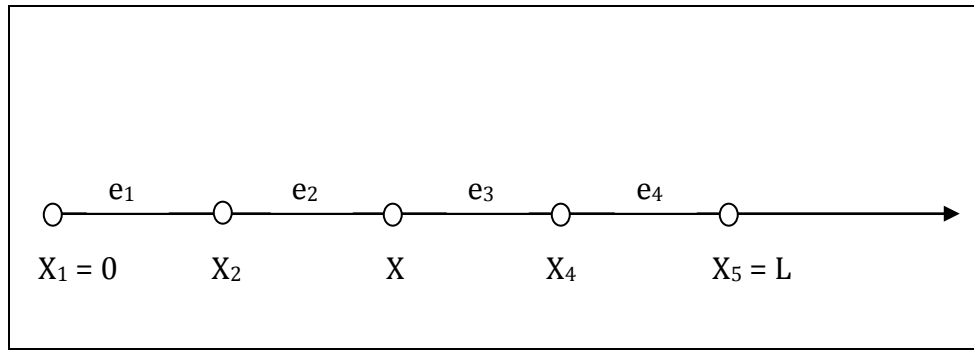


**Figure 4** One-Dimensional Finite-Element Mesh

In two dimensions, the domain  $\Omega$ , over which the heat-conduction equation is to be solved must be subdivided into elements of simple geometric shape. The simplest two-dimensional elements are based on triangles; however, there are advantages to using quadrilateral elements, especially because they offer better accuracy [3].

## 2.5

### Boundary Element Method

The boundary element method (BEM) is a well-established numerical technique for the solution of many engineering problems. It departs from an integral equation derived from the original partial differential equation describing the problem. The integral equation relies on Greens' free space solution to the adjoint differential equation operator and usually involves only boundary values of the field variable and its normal derivative. In the case of heat transfer the field variable is temperature and its normal derivative is related to the heat flux through the Fourier law of heat conduction. The discretization of the integral equation is thus confined to the boundaries of the region and dimensionality of the problem is thus reduced by one [3]. For example, an equation governing a three-dimensional region is transformed into one over its surface.

## 2.6

### Meshless Methods

For decades, the finite-element (FEM) and the finite-difference (FDM) methods have been the dominant numerical schemes employed in most scientific computation. These methods have been used to solve a wide range of technical problems from aircraft and auto design to medical imaging. Even so, there are often substantial changes in applying these techniques, particularly for complicated geometries and three-dimensional problems [3]. A considerable amount of time is needed to discretize and index the domain elements and this is still far from being fully automated, particularly in 3D. BEM presents an advantage in this area, whereas

only boundary discretization is required rather than domain discretization. However, it involves sophisticated mathematics beyond FEM and FDM and some difficult numerical integration of singular functions. In addition, all these traditional methods are often slowly convergent, frequently requiring the solution of thousands of equations to get acceptable accuracy.

Meshless methods use the geometry of the simulated object directly for calculations and do not rely on discretization. Neither domain nor surface meshing is required during the solution process. Recently, advances in the development and application of meshless techniques show they can be strong competitors to the more classical FEM and FDM approaches [17]. For instance, the meshless method only requires that one places nodes throughout the physical geometry thus the boundary is represented by a set of nodes, as opposed to creating a mesh. On the contrary, meshless methods require more CPU time since the creation of shape functions is more time-consuming and is performed during the computation.

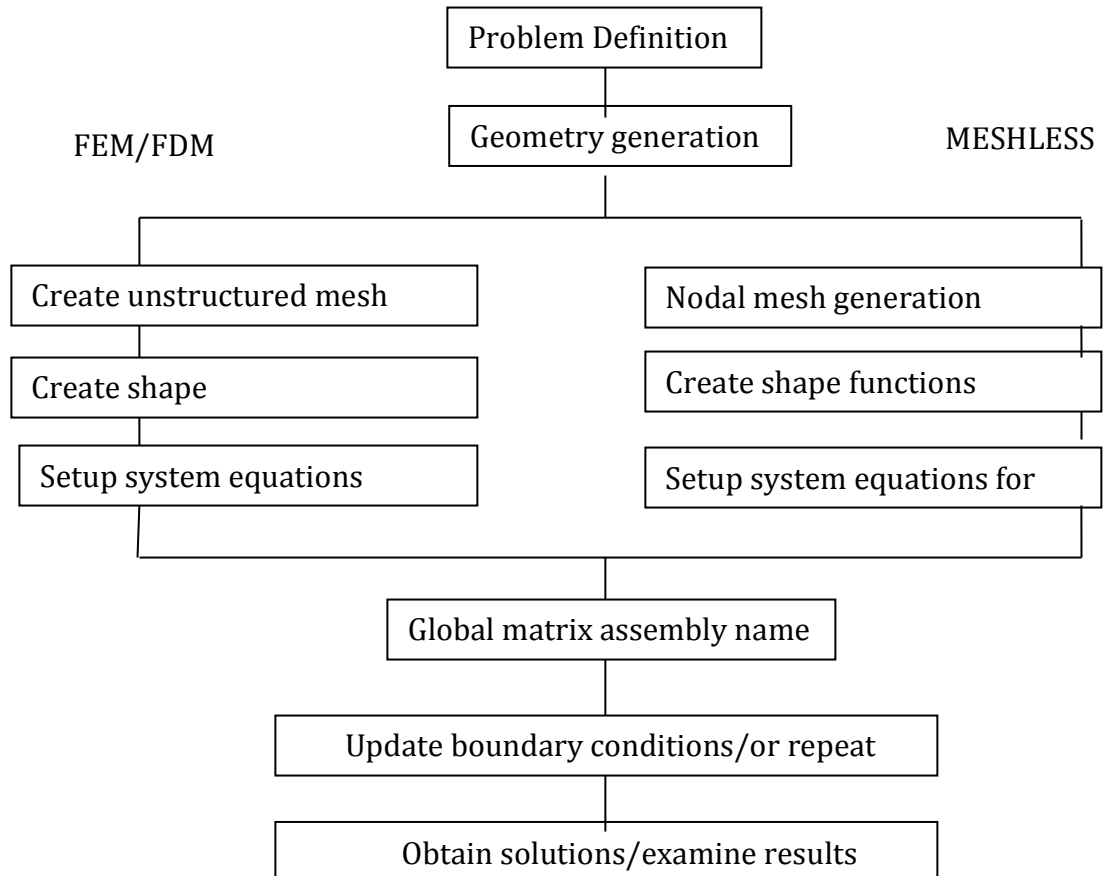


**Figure 5** Difference between FDM/FEM and Meshless Methods

Note that, although the meshless method may be more accurate than FDM/FEM techniques, it can be much slower with regard to computational time to achieve convergence. This is due, in part, to use of numerical integration and subsequent use of a direct matrix solver. However, meshless methods do not need any pre-knowledge of their nodal arrangement, as in conventional numerical schemes. This makes the method particularly attractive for developing adaptive capabilities.

## CHAPTER 3

### METHOD

An experiment was conducted by running a sample of fifty tests at various set-points. All the tests ran in a similar environment and a recording of temperature versus time was made once every thirty seconds. Below is a figure of a typical specimen sample used.

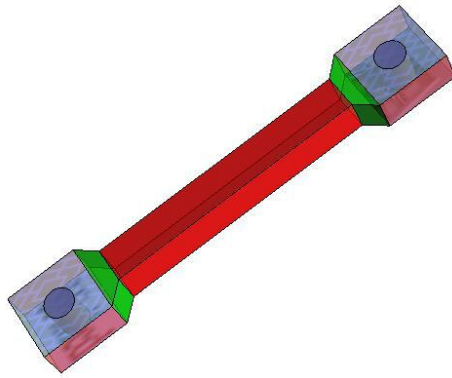


**Figure 6** Specimen Sample

For each recording temperature of, both the furnace and the dummy sample were measured at three different locations and the average of those readings were used in the study. We solve for the diffusivity coefficient of the material sample by fitting a curve to the measured specimen reading where the two-dimensional heat equation is the theoretical governing model. For simplicity, the governing equation is discretized on a rectangular domain with equal spacing in both  $x$  and  $y$  direction. The figure below shows a typical nodal grid used throughout this thesis. The fine grid section in the middle represents the solid material for which we are investigating and the surrounding region is for the ambient air temperature.

By discretizing the two-dimensional heat equation we solve the resulting system of linear equations where each node on the grid represents an equation

relating the temperature at node  $(i, j)$  to its immediate surrounding depending on the scheme used. For the five-point scheme, node  $(i, j)$  is related to nodes  $(i + 1, j), (i - 1, j), (i, j + 1), (i, j - 1)$ . For the nodes at the edge, including the corners, we use the boundary contribution for the missing nodes.

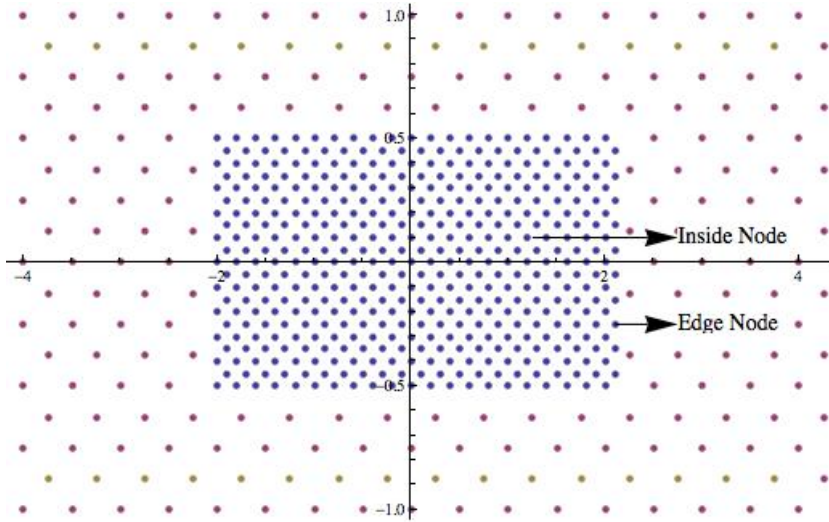


**Figure 7** 2D Nodal Grid

After formatting the grid, we initialize it and specify boundary conditions on all four sides of the grid. A complete initialization consists of the following:

- Initial temperature at time  $t = 0$
- $\Delta t$
- $dx$
- Final time
- Boundary temperature at final time
- Number of iterations: calculated as  $(\text{final time} - \text{initial time})/\Delta t + 1$

Below is a figure of a grid initialized to 75 degrees at time zero.

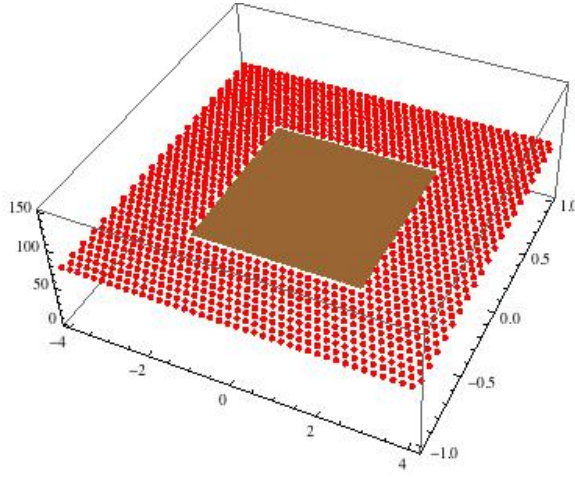


**Figure 8** Initialized 2D Nodal Grid

Once the problem has been initialized, we pick an initial guess for the value of alpha and confirm that  $(\alpha * \Delta t)/dx^2 \leq 0.25$ . This is the stability constraint for a two-dimensional heat transfer under the simple explicit scheme [3]. We chose to keep  $dx$  fixed and adjust  $\Delta t$  in order to meet the stability constraint. Here  $\alpha$  is the diffusivity coefficient. The boundary setting is determined by interpolating the furnace temperature as a function of time. The simulation is run for various small time increments, and the resulting simulation curve is compared against the true specimen temperature versus time curves. The value of  $\alpha$  is increased when simulation curve falls below the specimen curve. Otherwise,  $\alpha$  is decreased. It is important to check the stability constraint as  $\alpha$  is increased, adjusting  $\Delta t$  as needed. The code has a reminder to perform this check.

As we iterate solving  $A x = b$ ,  $A$  being the sparse matrix representing the chosen scheme, special attention is required as to how column  $b$  is to be updated. First, the solution column,  $x$ , is distributed back into the correct  $(i, j)$  position and this is multiplied by matrix  $A$ . This is equivalent to propagating temperature through space. Vector  $b$  is then set to the previous  $b$  plus the result of this matrix

multiplication plus the boundary contribution added on to count for the missing  $(i, j-1)$ ,  $(i+1, j)$ ,  $(i, j+1)$  and  $(i-1, j)$  nodes at the domain edges. With column b updated, we continue looping through time and space until convergence or maximum number of iterations is achieved. Convergence in our case is realized by comparing successive differences of temperature profiles to a predetermined small threshold. In effort to save time and memory space, due to solving  $A x = b$  repeatedly, it was observed that by zeroing actual temperature and plotting it against elapsed time, we are indeed

plotting  $\frac{\partial u}{\partial t}$ . So in essence once discretized in space and time,  $u_t = \alpha(u_{xx} + u_{yy})$  is

transformed into the resulting ODE system,

$\frac{\partial u}{\partial t} = \frac{1}{\Delta x^2} A u$ , where A is our sparse matrix and u is the boundary conditions. This

does not need to be solved for  $u$  but for  $\frac{\partial u}{\partial t}$  because we are interested in comparing

the actual temperature curve versus experimental curve. Since actual temperature

curve is given by  $\frac{\partial u}{\partial t}$ , we only perform  $\frac{1}{\Delta x^2} A u$  to obtain the experimental temperature

curve.

Another critical point to remark in our method is the boundary contribution to the edge nodes as we iterate through time and space. This amount is considered inversely proportional to the squared distance between the boundary and the edge nodes and directly proportional to time. For those nodes inside the domain, i.e not on the edge, this contribution is set to zero.

### 3.1

#### Results

Select a data sample from the collected temperature versus time experimental data and plot the temperature versus time for both the furnace and the material. Using file "N90663\_Data.mat" here is the plot obtained. The connected line is for the furnace while the dotted line is for the material sample.

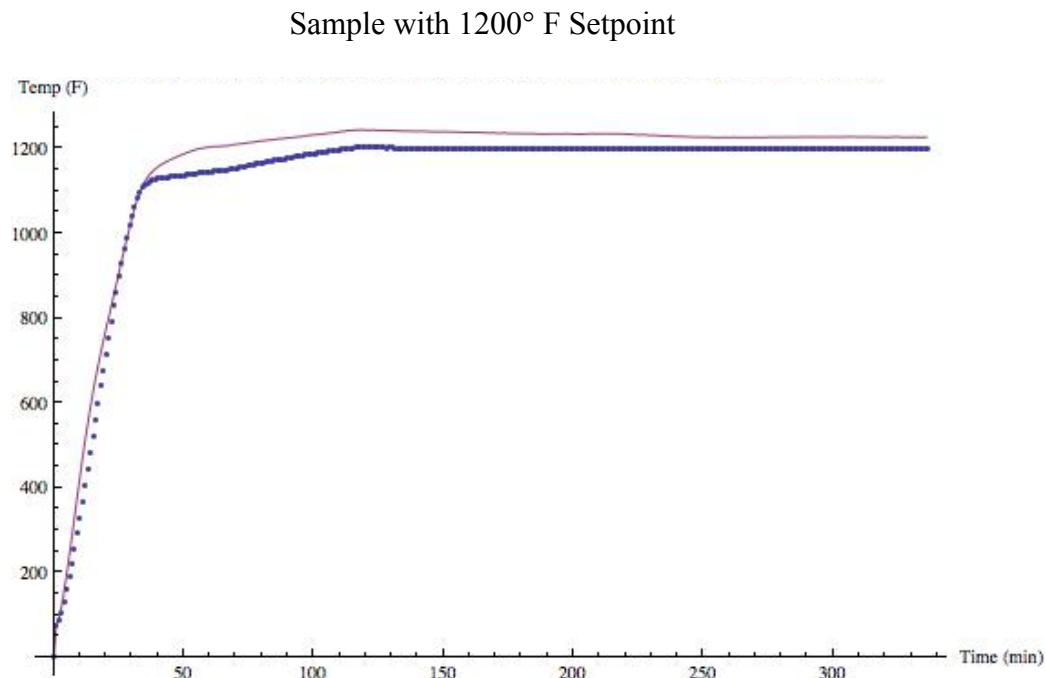
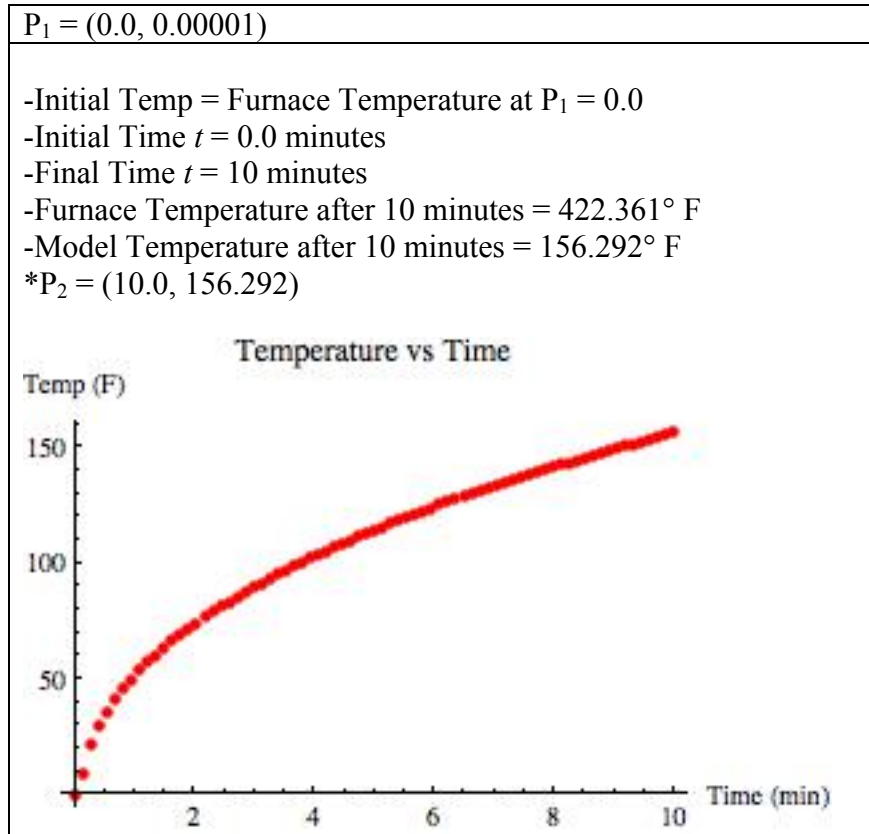


**Figure 9** Temperature vs Time Plot of an Experimental Test

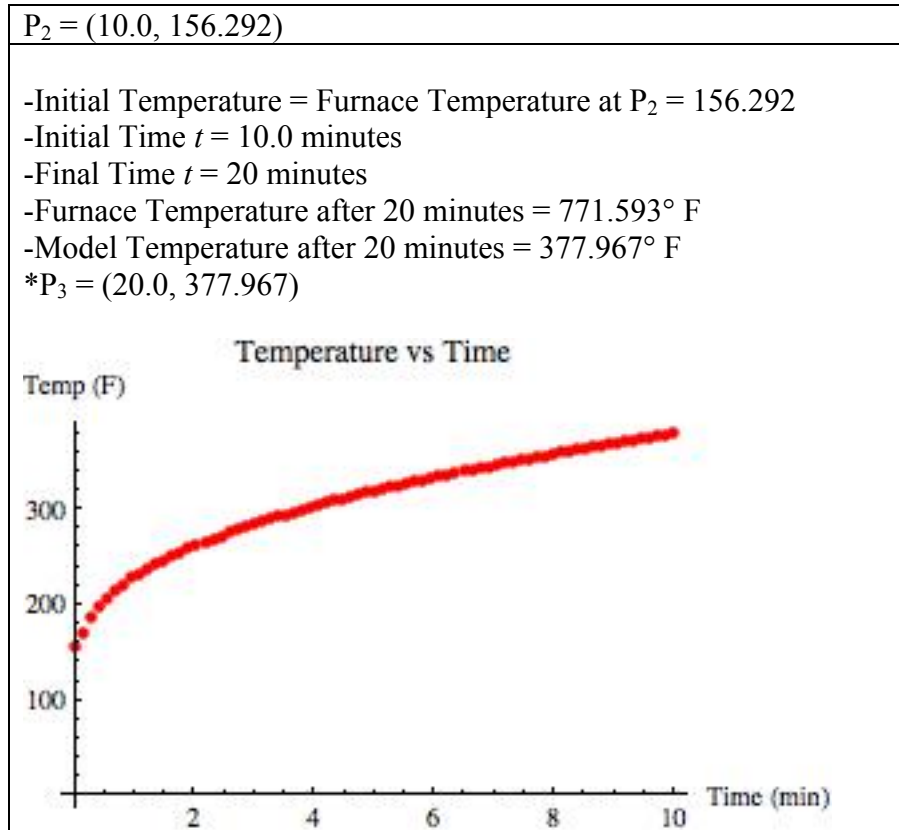
The claim in this thesis is that given such information, we ought to be able to retrieve the diffusion coefficient of this material. We use the furnace information to initialize the boundary and solve for  $\alpha$  that gives us a reasonable fit to the curve for the experimental data. With the problem initialized and boundary values set, a time interval of ten minutes is used and the table below shows how we would go about determining the first three curve fit points.

**Table 1** Model output for  $\alpha = 0.016563$ ,  $\Delta t = 0.135$ ,  $dx = 0.1$  for the first point



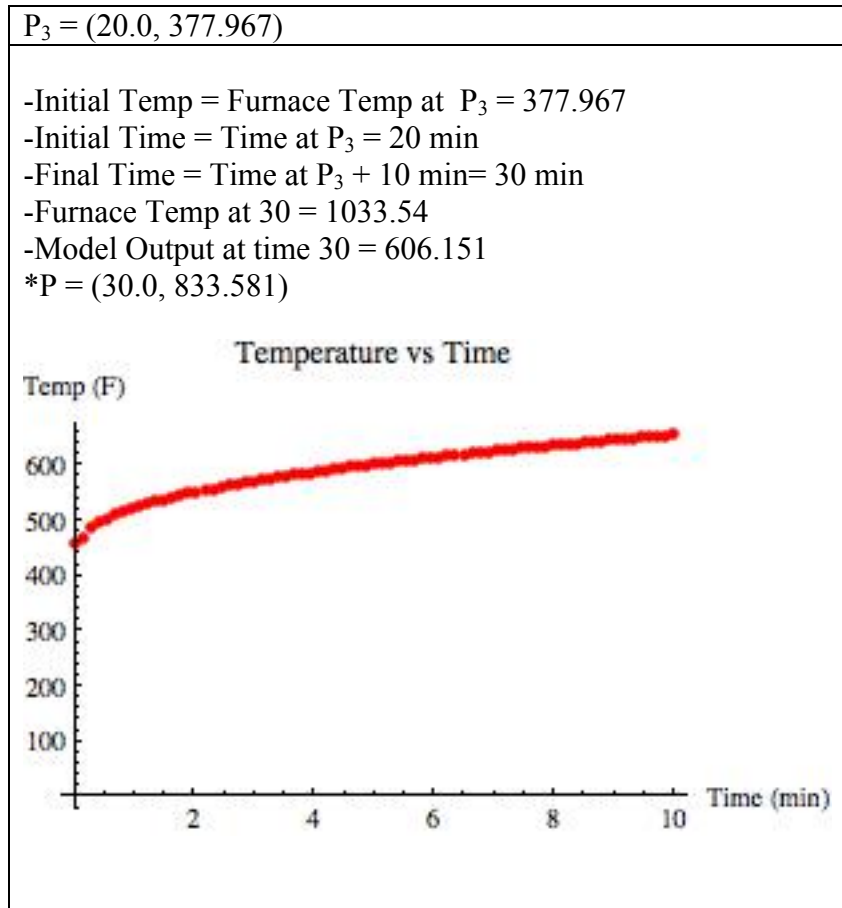
At  $P_1$ , an initial guess for  $\alpha$  is used and we pick a small  $\Delta t$  and  $dx$  such that the stability constraint for the model is satisfied. Record model output after running the model for ten minutes. Note that the furnace temperature at ten minutes is obtained from the data. Thereafter,  $P_2(t_1, y_1)$  is obtained where  $t_1$  and  $y_1$  represent time and model temperature at  $P_1$ .

**Table 2** Model output for  $\alpha = 0.016563$ ,  $\Delta t = 0.135$ ,  $dx = 0.1$  for the second point



At  $P_2$ , we initialize the model with output from  $P_1$ . Initial time is set to ten minutes and the initial furnace temperature is obtained from the data at time  $t = 10$ . Record model output after running the model for ten minutes. Thereafter,  $P_3(t_2, y_2)$  is obtained where  $t_2$  and  $y_2$  represent time and model temperature at  $P_2$ . Similarly, this process is continued for subsequent points and table 4 shows the results.

**Table 3** Model output for  $\alpha = 0.016563$ ,  $\Delta t = 0.135$ ,  $dx = 0.1$  for the third point



Extending the example above, we show the results obtained from calculating the first nine points of our curve fit. The effect of increasing the  $\alpha$  value is obtained by calculating the percent relative error. Also, for each case study, a plot showing the resulting simulation or model curve is displayed along with the specimen or actual curve.

Case 1:

Data File = "N90663\_Data.mat"

$\alpha = 0.016563, 0.018, 0.018519$

$$dx = 0.1$$

$$\Delta t = 0.135$$

The table below contains the results of running the simulation model with the above parameters

**Table 4** Five-Point Scheme with  $\Delta t = 0.135$

Time (minutes)	Furnace Temperature (°F)	Specimen Temperature (°F)	Model output @ a = 0.016563	Model output @ a = 0.018	Model output @ a = 0.018519
0.0	0.00001	0.00001	0.00001	0.00001	0.00001
10.0	422.361	328.025	156.292	161.123	162.815
20.0	771.593	710.931	377.967	387.269	390.45
30.0	1033.54	1039.12	606.151	617.614	621.466
40.0	1156.6	1129.68	786.818	797.399	800.875
50.0	1187.27	1136.41	905.169	912.78	915.187
60.0	1203.59	1145.43	981.303	985.546	986.78
70.0	1210.02	1153.89	1028.77	1029.96	1030.16
80.0	1218.13	1166.5	1059.89	1058.67	1058.06

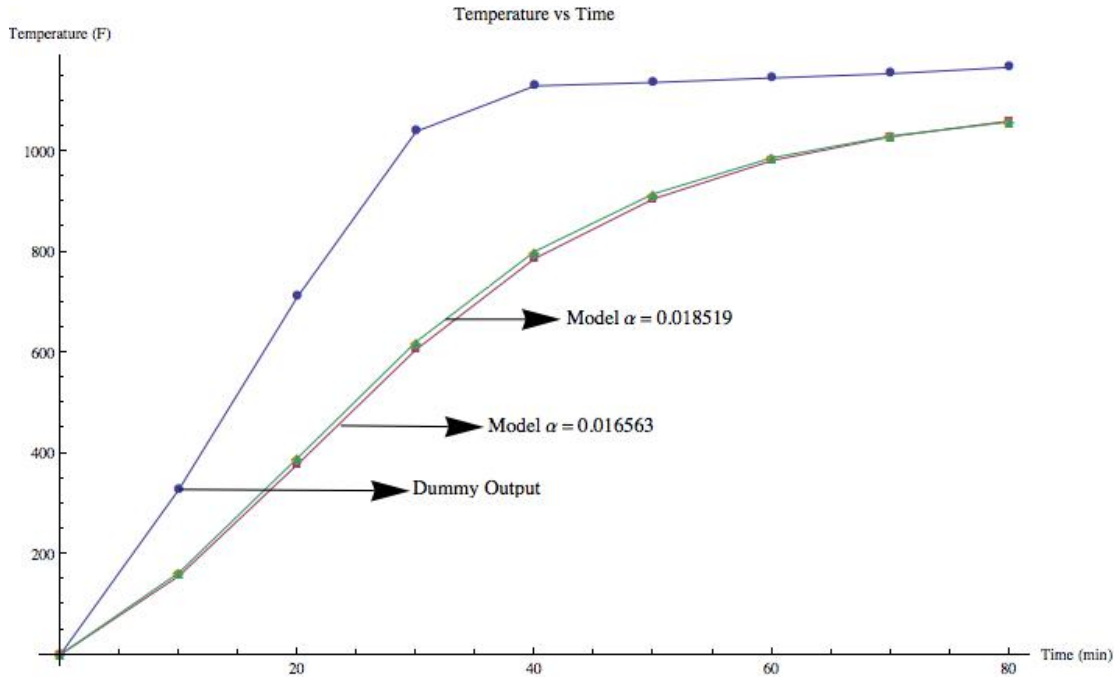


**Figure 10** Temperature vs Time Plot for Five-Point Scheme with  $\Delta t = 0.135$

**Table 5** Five-Point Scheme with  $\Delta t = 0.02$ . Contains the results of running the simulation model with parameters given in Case 2 below

Time	Furnace Temperature	Specimen Temperature	Model output @ a = 0.10950	Model output @ a = 0.11750
0.0	0.00001	0.00001	0.00001	0.00001
10.0	422.361	328.025	318.663	323.247
20.0	771.593	710.931	637.091	640.99
30.0	1033.54	1039.12	889.622	891.072
40.0	1156.6	1129.68	1026.01	1024.3
50.0	1187.27	1136.41	1072.66	1068.57
60.0	1203.59	1145.43	1093.02	1087.97
70.0	1210.02	1153.89	1101.38	1095.92
80.0	1218.13	1166.5	1108.94	1103.37

Case 2:

Data File = "N90663\_Data.mat"

$\alpha = 0.10950, 0.11750$

$dx = 0.1$

$\Delta t = 0.02$

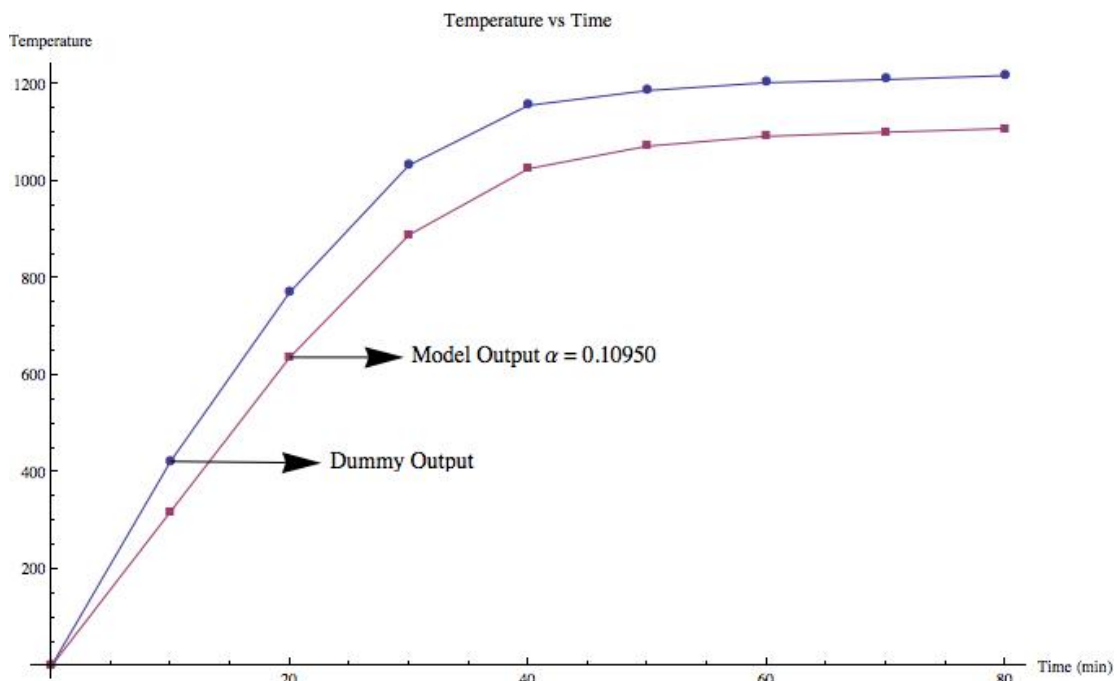


**Figure 11** Temperature vs Time Plot for Five-Point Scheme with  $\Delta t = 0.02$

### 3.2

#### Conclusion

We showed how given temperature behavior of a homogeneous metal alloy over time, an inverse heat transfer problem can be formatted to solve for the diffusivity coefficient of the alloy. By discretizing Fourier's law in two dimensions over a rectangular domain with equal spacing both in  $x$  and  $y$  direction, the problem was transformed into a system of linear equations with each node represented by a

single equation. This resulted in a large nonsingular symmetric sparse matrix. An explicit time stepping method is used and a series of curves is constructed to approximate the actual measured sample curve. Each resulting model curve is a function of  $\alpha$  and is subject to a stability constraint imposing that  $\frac{\alpha \Delta t}{dx^2} \leq 0.25$ . It is  $\alpha$ , the diffusivity coefficient, which we are seeking to uncover.

While explicit stepping methods are bounded to smaller  $\Delta t$ , depending on the  $\alpha$  value, we overcome this by fitting the curve in small time ranges. The case studies shown in the results section use a time interval of ten minutes. Thus, we update the curve fit every ten minutes. Therefore the initial and boundary conditions are adjusted accordingly before approximating over the subsequent interval. Boundary conditions are set locally to the furnace reading at time  $t + 1$  and the initial condition is associated with the simulated/model output at time  $t$ . This reduced the number of iterations significantly and also storage. Meanwhile, since matrix  $A$  is fixed, we utilized a `LinearSolve[...]` function procedure to facilitate solving  $A x = b$  for numerous  $b$ . Documentation for the `LinearSolve[...]` procedure can be found in Mathematica' documentation.

Although the most accurate diffusivity coefficient approximation would be associated with finding a highly accurate fit to the experimental data, the results obtained here are still usable in terms of minimizing the total ramping time. This is accomplished by dynamically determining the material response to its surrounding and adjusting control parameters for the next short time interval. The length of this interval is dependent upon to available computing infrastructure. Note that by

incorporating some of the suggested approaches here such as cloud, parallel or grid computing, more accuracy can be achieved.

### 3.3

#### Endnotes

By investigating computational determination of  $\alpha$ , we have in essence provided a framework to tackle the more challenging and meaningful problem of furnace temperature control in material testing. For a given material alloy, we consider ramping its temperature to a particular set-point in the minimum possible time without a temperature overshoot outside of acceptable bounds. We need a robust learning algorithm to utilize the heat diffusivity knowledge learned from this thesis and provide a control mechanism that minimizes ramping time. Once this is obtained, the algorithm can be adapted to run in real time.

In the meantime, refinement of the current model is needed in terms of our domain discretization process and weight function. Mesh representation of our furnace and the metal alloy remain one of the most intriguing processes. This is still a big open area for improvement in the future work on this project. Consideration of meshless methods as described in chapter two, might aid real-time computation. Also, a systematic method of picking the initial  $\alpha$  guess would speed up the curve-fitting process. On the other hand, in terms of the model discretization, alternating directions implicit method (ADI) is going to be considered. In this method, resulting equations to be solved in each step have a simpler structure and can be solved efficiently with tridiagonal matrix algorithm. We acknowledge that Crank-Nicolson method is a very competitive method to be considered, but it results in a complicated set of equations

to be solved—especially in higher dimensions. This added cost in Crank-Nicolson makes ADI method even more attractive for future improvements.

## REFERENCES

- [1] J. Hadamard, Lectures on Cauchy's Problem in Linear Differential Equations, Yale University Press, New Haven, CT, 1993.
- [2] O.M. Alifanov, Inverse Heat Transfer Problems, Springer-Verlag, Berlin, 1994.
- [3] W.J Minkowycz, E.M. Sparrow, J.Y. Murthy, Handbook of Numerical Heat Transfer, John Wiley & Sons, Inc., Hoboken, New Jersey, 2006.
- [4] A.N. Tikhonov, Solution of Ill-posed Problems, Halsted, Washington, DC, 1977.
- [5] J. V. Beck, B. Blackwell, S.R. St. Clair, Jr., Inverse Heat Conduction Problems. John Wiley and Sons, New York, 1985.
- [6] H.J. Reinhardt, Analysis of sequential methods solving the inverse heat conduction problem, Numerical Heat Transfer, Part B, vol. 24, pp. 445-474. (1993).
- [7] J. P. Kaipio and E. Somersalo, Computational and Statistical Methods for Inverse Problems, Springer-Verlag, Berlin, 2004.
- [8] A. F. Emery, A. V. Nenarokomov, and T.D. Fadale, Uncertainties in Parameter Estimator: The Optimal Experimental Design, Int. J. Heat Mass Transfer, 43, 3331-3339 (2002).
- [9] A. F. Emery, B. F. Blackwell, and K. J. Dowling, The Relationship Between Information, Sampling Rates, and Parameter Estimation Model, ASME J. Heat Transfer, 124, 1192-1199 (2003).
- [10] C. P. Robert, The Bayesian Choice, From Decision-Theoretic Foundations to Computational Implementation, 2nd ed., Springer-Verlag, New York, 2001.

- [11] J. Wang and N. Zabaras, A Bayesian Inference Approach to the Stochastic Inverse Heat Conduction Problem, *Int. J. Heat Mass Transfer*, 47, 3927-3941 (2004).
- [12] C. Andrieu, N. Freitas, A. Doucet, and M. Gordon, An Introduction to MCMC for Machine Learning, *Mach. Learning*, 50, 5-43 (2003).
- [13] M. Turner, R. W. Clough, H. H. Martin and L. Topp, Stiffness and Deflection Analysis of Complex Structures, *J. Aero. Sci.*, 23, 805-823 (1956).
- [14] E. L. Wilson and R. E. Nickel, Application of the Finite Element Method to Heat Conduction Analysis, *Nucl. Eng. Design*, 4, 276-286 (1996).
- [15] R. D. Cook, D. S. Malkus, M. E. Plesha, and R. J. Witt, *Concepts and Applications of Finite Element Analysis*, Wiley, New York, 2002.
- [16] B. A. Finlayson, *The Method of Weighted Residuals and Variational Principles*, Academic Press, New York, 1972.
- [17] R. W. Lewis, K. Morgan, H. R. Thomas, and K. N. Seetharamu, *The Finite Element Method in Heat Transfer Analysis*, Wiley, Chichester, UK, 1996.
- [18] R.A Gingold and J.J. Monaghan, Smoothed Particle Hydrodynamics: Theory and Application to Non-spherical Stars, *Mon. Not. R. Astron. Soc.*, Vol 181, pp. 375-89, 1977.
- [19] G. R. Liu, *Mesh Free Methods: Moving Beyond the Finite Element Method*, CRC Press, Boca Raton, FL, 2002.
- [20] S. N. Atluri and T. Zhu, A New Meshless Local Petrov-Galerkin (MLPG) Approach in Computational Mechanics, *Comput. Mech.*, 22, 117-127, 1998.

- [21] M.D. Buhmann, Radial Basis Functions: Theory and Implementations, Cambridge University Press, 2003.
- [22] M. J. D. Powell, The Theory of radial basis function in 1990, in W. Light (ed.), Advances in Numerical Analysis, Vol. II, pp. 105-210, Oxford Sci. Pub., Oxford, UK, 1992.
- [23] E. J. Kansas, Multiquadratics - A Scattered Data Approximation Scheme with Applications to Computational Fluid Dynamics II, Comput. Math. Appl., 19, 147 161 (1990).
- [24] D. W. Peaceman and H. H. Rachford, The Numerical Solution of Parabolic and Elliptic Differential Equations, J. Soc. Ind. Appl. Math., 3, 28-41 (1955).
- [25] J. Douglas, On the Numerical Integration of  $\frac{\partial^2 u}{\partial x^2} + \frac{\partial^2 u}{\partial y^2} = \frac{\partial u}{\partial t}$  by Implicit Methods, J., Soc. Ind. Appl. Math., 3, 42-65 (1955).
- [26] G. Timothy, B.G. June, L. Imre., The Princeton Companion to Mathematics, Princeton University Press, 2008.
- [27] M. A. Larussa, I. Knowles., Conditional Well-posedness for an Elliptic Inverse Problem, SIAM J. Appl. Math. Vol. 71. No. 4, pp. 952-971.
- [28] A. Iserles, A First Course in the Numerical Analysis of Differential Equations, 2nd ed., Cambridge University Press, 2009.
- [29] L. V. Ahlfors., Complex Analysis, 3rd ed, International Series in pure and Applied Mathematics, MacGraw-Hill, Inc, 1979.
- [30] Y. Chen, M.Xia, D.Wang, D. Li., Application of Radial Point Interpolation Method to Temperature Field, Journal of Mathematics Research, Vol., 2, No. 1, February 2010.

- [31] R. Bank and T. Dupont, An Optimal Order Process for Solving Finite Element Equations, *Math. Comp.*, 36 (1981), pp. 35-51.
- [32] J. Bramble, J. Pasciak, and J. Xu, The Analysis of Multigrid Algorithms with Non-nested Spaces or Non-Inherited Quadratic forms, *Math. Comp.*, 56 (1991), pp.1-34.
- [33] A. F. Emery, Stochastic Regularization for Thermal Problems with Uncertain Parameters, *Inverse Problems Eng.* 9, 109-125 (2001).
- [34] J. Wang and N. Zabaras, A Bayesian Inference Approach to the Stochastic Inverse Heat Conduction Problem, *Int. J. Heat Mass Transfer*, 47, 3927-3941 (2004).
- [37] J.H. Wilkinson, The Algebraic Eigenvalue Problem, *Math. Comp.*, 20 (1965), pp. 621-635.
- [38] W. H. Liu and A. H. Sherman., Comparative Analysis Of The Cuthill-McKee and The Reverse Cuthill-McKee Ordering Algorithms For Sparse Matrices, *SIAM J. Numer. Anal.* Vol 13, No 2 (Apr. 1976), pp.198-213.
- [39] E. Cuthill and J.McKee., Reducing The Bandwidth Of Sparse Symmetric Matrices, *ACM New York, NY, USA* (1969).
- [40] A. Lim, B. Rodrigues and F. Xiao., A Centroid-based Approach To Solve the Bandwidth Minimization Problem, Proceedings of the 37<sup>th</sup> Hawaii International Conference on System Sciences, 2004.